Journal of Chromatography A, 1218 (2011) 484–490

Contents lists available at ScienceDirect

Journal of Chromatography A

journal homepage: www.elsevier.com/locate/chroma

A novel adsorbent for protein chromatography: Supermacroporous monolithic cryogel embedded with Cu^{2+}-attached sporopollenin particles

Mahmut Erzengin, Nuri Ünlü, Mehmet Odabaşı*

Aksaray University, Faculty of Arts and Science, Chemistry Department, Aksaray, Turkey

ARTICLE INFO

Article history:
Received 20 July 2010
Received in revised form 8 November 2010
Accepted 29 November 2010
Available online 5 December 2010

Keywords:
Protein adsorption
Cryogels
Sporopollenin
Metal chelate
Particle embedding

ABSTRACT

The aim of this study is to prepare supermacroporous cryogels embedded with Cu^{2+}-attached sporopollenin particles (Cu^{2+}-ASP) having large surface area for high protein adsorption capacity. Supermacroporous poly(2-hydroxyethyl methacrylate) (PHEMA)-based monolithic cryogel column embedded with Cu^{2+}-ASP was prepared by radical cryo-copolymerization of 2-hydroxyethyl methacrylate (HEMA) with *N*,*N*′-methylene-bis-acrylamide (MBAAm) as cross-linker directly in a plastic syringe for affinity purification of human serum albumin (HSA). Firstly, Cu^{2+} ions were attached to sporopollenin particles (SP), then the supermacroporous PHEMA cryogel with embedded Cu^{2+}-ASP was produced by free radical polymerization using *N*,*N*,*N*′,*N*′-tetramethylene diamine (TEMED) and ammonium persulfate (APS) as initiator/activator pair in an ice bath. Embedded particles (10 mg) in PHEMA-based cryogel column were used in the adsorption/desorption of HSA from aqueous solutions. Optimum conditions of adsorption experiments were performed at pH 8.0 phosphate buffer, with flow rate of 0.5 mL/min, and at 5 °C. The maximum amount of HSA adsorption from aqueous solution was very high (677.4 mg/g SP) with initial concentration 6 mg/mL. It was observed that HSA could be repeatedly adsorbed and desorbed to the embedded Cu^{2+}-ASP in PHEMA cryogel without significant loss of adsorption capacity.

1. Introduction

Albumin has played an important role in the fluid management of acutely ill patients for more than 50 years. Some examples in the United States for licensed albumin therapy such as hypovolemia of shock, burns, hypoalbuminemia, cardiopulmonary bypass, hemodialysis, hyperbilirubinemia, sequestration of protein-rich fluids in acute peritonitis and extensive cellulitis have been summarized elsewhere [1]. Research on albumin separation has attracted considerable attention for its great potential in blood protein manufacture. Human serum albumin is isolated from human plasma by Cohn's method [2]. This method concerns the precipitation of proteins using ethanol with varying pH, ionic strength and temperature. However, this technique, which is the oldest method of industrial fractionation of proteins, is not highly specific and can give partially denaturated proteins [3]. Hence it is important to use cheap and efficient techniques for the removal of albumin. In respect of ease preparation, economy, adsorption capacity and stability, immobilized metal affinity chromatography (IMAC) offers several advantages when compared to other types of affinity chromatography, in particular immunoaffinity chromatography, e.g., ligand stability and protein loading [4–7]. IMAC is a sensitive technique for protein separation that enables distinguishing between proteins differing by only a single histidine residue on the surface [8–10]. Proteins interact mainly through the imidazole group of histidine and, to a lesser extent, the indoyl group of tryptophan and the thiol group of cysteine. Aromatic amino acids and the amino terminals of the peptides also contribute to retention of the protein in IMAC [11]. The low cost of metals and the ability to reuse adsorbents hundreds of times without any detectable loss of metal-chelating properties are the attractive features of metal affinity separation.

Sporopollenin obtained from *Lycopodium clavatum* is a natural biopolymer that has a constant chemical structure and contains only carbon, hydrogen and oxygen. It is highly resistant to both biological decay and chemical attack. It has a high capacity, and occurs naturally as a component of spore walls [12]. Architecturally, spores and pollen membranes have two layers, an inner one known as intine, made of cellulose and polysaccharides, and an outer one (exine) composed of a substance known as sporopollenin. Due to the constant mesh size, ready commercial availability, and constant molecular structure of sporopollenin, it has important

* Corresponding author at:Aksaray University, Faculty of Arts and Science, Chemistry Department, Biochemistry Division, 68100 Aksaray, Turkey.
Tel.: +90 382 280 1216; fax: +90 382 280 1249.
E-mail address: modabasi@aksaray.edu.tr (M. Odabaşı).

0021-9673/$ – see front matter © 2010 Elsevier B.V. All rights reserved.
doi:10.1016/j.chroma.2010.11.074

advantages over synthetic resins [13]. Infra-red and ^{13}C NMR spectroscopic studies on sporopollenin derived from pteridophyta and spermatophyta have shown that sporopollenin has aliphatic, aromatic, hydroxyl, carbonyl/carboxyl and ether functions in various portions in its polymeric structure [14].

Cryogels are known as a novel generation of stationary phases in the separation science [15,16]. Cryogels which have several advantages such as large pores, short diffusion path, low pressure drop, and very short residence time for both adsorption and elution are a very good alternative to purification of biomolecules [17]. However, the adsorption capacity of the cryogels for proteins is low due to the interconnected supermacropores within the matrix (i.e., low surface area) [18,19]. Improving the binding capacity of supermacroporous cryogels has a great importance in a bioseparation process [20,21].

In this study, a novel continuous supermacroporous monolithic cryogel embedded with Cu^{2+}-ASP having large surface area for high protein adsorption capacity was prepared under the freezing-temperature. Pore structure and morphology of the embedded particles in the cryogel were studied by scanning electron microscopy (SEM).

2. Methods and materials

2.1. Materials

Hydroxyethyl methacrylate (HEMA) was obtained from Fluka A.G. (Buchs, Switzerland), distilled under reduced pressure in the presence of hydroquinone inhibitor, and stored at 4 °C until use. *N*,*N*′-methylene-bis-acrylamide (MBAAm) and ammonium persulfate (APS) were supplied by Sigma (St. Louis, MO, USA). All other chemicals were of reagent grade and were purchased from Merck AG (Darmstadt, Germany). *L. clavatum* spores (sporopollenin) with 20 μm particle size mesh and *N*,*N*,*N*′,*N*′-tetramethylethylenediamine (TEMED) were obtained from Fluka A.G. (Buchs, Switzerland). Human serum albumin (HSA, 98% pure by gel electrophoresis, fatty-acid free, 67 kDa) was purchased from Aldrich (Munich, Germany). Coomassie Blue, for the Bradford Protein Assay, was obtained from BioRad (Richmond, CA, USA). Water used in the experiments was purified using a Barnstead (Dubuque, IA, USA) ROpure LP® reverse osmosis unit with a high-flow cellulose acetate membrane (Barnstead D2731), followed by a Barnstead D3804 NANOpure® organic/colloid removal and ion-exchange packed bed system.

2.2. Preparation of sporopollenin particles

10 g of *L. clavatum* spores was refluxed with 75 mL of acetone for 4 h to remove the hydrophobic layer, i.e., fat, to increase the hydrophilicity of the resin. The defatted spores were also treated with 2.0 M NaOH for 24 h to remove lignin like structure. After filtration, the sporopollenin residue was washed with hot water (150 mL) 5 times and then with hot ethanol 2 times, and dried at 60 °C under vacuum. The remaining membrane portion (sporopollenin) was used for further applications.

2.3. Preparation of Cu^{2+}-attached sporopollenin particles (Cu^{2+}-ASP)

The optimized adsorption conditions of Cu^{2+} onto sporopollenin particles (SP) were performed as described previously [22]. Briefly, 0.150 g of SP was treated with a Cu^{2+} solution [150 mg/L (pH 5.0), adjusted with HCl and NaOH] at room temperature for 2 h. A 1000-ppm atomic absorption standard solution was the source of the Cu^{2+} ions. The concentration of the Cu^{2+} ions in the resulting solution was determined with a graphite furnace atomic absorption spectrometer (GFAAS, Analyst 800/PerkinElmer, USA). The instrument response was periodically checked with known metal solution standards. The experiments were performed in triplicate. The Cu^{2+} concentrations in the initial and final solutions were used to calculate the amount of Cu^{2+} ions adsorbed.

Cu^{2+} leakage from the Cu^{2+} loaded SP was investigated in media whose pH varied between 4.0 and 7.0 and also in a medium-containing 1.0 M NaCl. The monolith was stirred for 24 h at room temperature. Then the concentration of Cu^{2+} ions in the supernatants was determined using an atomic absorption spectrophotometer.

2.4. Preparation of Cu^{2+}-attached sporopollenin particle embedded cryogel (Cu^{2+}-ASPEC) column

Preparation of supermacroporous monolithic cryogel embedded with Cu^{2+}-ASP is described as follows.

Monomers (50 mg MBAAm and 0.3 mL HEMA) were dissolved in deionized water (5 mL) and the mixture was degassed under vacuum for about 5 min to eliminate soluble oxygen. The cryogel was produced by free radical polymerization initiated by TEMED (20 μL) and APS (100 μL) (10%, w/v). After adding APS, the solution was cooled in an ice bath for 2–3 min. TEMED was added and the reaction mixture was stirred for 1 min. In this step, 10 mg of Cu^{2+}-ASP was added to the polymerization mixture. Then, the reaction mixture was poured into a plastic syringe (5 mL, i.d. 0.8 cm). The polymerization solution in the syringe was frozen at −12 °C for 24 h and then thawed at room temperature. For the removal of unconverted monomers and initiator, washing solutions (i.e., a dilute HCl solution and a water–ethanol mixture) were recirculated through the monolithic cryogel column, until cryogel column is clean. Purity of the monolithic cryogel was followed by observing the change of optical densities of the samples taken from the liquid phase in the recirculation system. After washing, the cryogel was stored in buffer containing 0.02% sodium azide at 4 °C until use. Illustration of cryogel embedded with Cu^{2+}-attached SP for HSA is represented in Fig. 1.

2.5. Characterization of cryogel

2.5.1. The porosity of Cu^{2+}-ASPEC column

For the measurement of volume and free water content of the cryogel sample, φ value was estimated. A piece of cryogel sample was saturated with deionized water, then it was immersed in water having volume V_1, after that the total volume of cylinder was measured as volume V_2. Water-saturated cryogel volume V_0 was calculated by the volume difference, i.e., $V_0 = V_2 - V_1$.

The mass of water-saturated cryogel, m_w, was weighted. After squeezing the cryogel sample to remove the free water within the large pores, the mass of the cryogel sample without free water, m_s, was weighted as described previously [20]. The porosity was calculated by the following formula:

$$\varphi = \frac{m_w - m_s}{\rho_w V_0} \quad (1)$$

where ρ_w is the density of deionized water. Then the cryogel sample was dried in the oven at 60 °C for 12–24 h to a constant and the dried cryogel mass m_d was determined, and the total water fraction (TWF) was calculated by the following formula:

$$\mathrm{TWF} = \frac{m_w - m_d}{\rho_w V_0} \quad (2)$$

2.5.2. Surface morphology

The morphology of a cross section of the dried cryogel was investigated by SEM. The sample was fixed in 2.5% glutaraldehyde

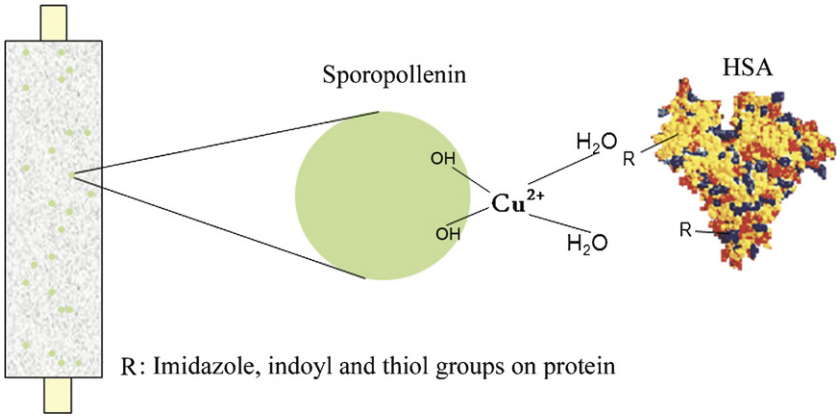

Fig. 1. Cryogel embedded with Cu^{2+}-attached SP for HSA.

in 0.1 M sodium phosphate buffer (pH 7.0) overnight. The sample was washed using the same buffer for three times and post-fixed in 1% osmium tetroxide for 1 h and re-washed. Then the dehydration of sample was performed using ethanol–water mixtures (0–25–50–75–99.5%). The dehydrated sample was transferred to a critical point drier, coated with gold–palladium (40:60) and examined using a JEOL JSM 5600 SEM (Tokyo, Japan).

2.6. Chromatographic procedures

2.6.1. HSA adsorption from aqueous solutions

HSA adsorption experiments onto Cu^{2+}-ASPEC column were carried out in a recirculating system equipped with a water jacket for temperature control. The cryogel was washed with 30 mL of water and then equilibrated with 0.02 M phosphate buffer (pH 8.0). Then the prepared HSA solution (i.e., 50 mL) was pumped through the column (column volume of 5 mL) under recirculation for 1 h. The adsorption was followed by monitoring the decrease in UV absorbance at 280 nm. The effects of HSA concentration, medium pH, flow rate and temperature on adsorption capacity were studied.

In all cases, HSA elution studies were performed using 0.05 M acetate buffer containing 1 M NaCl (pH 5.0). In a typical desorption experiment, 30 mL of desorption agent was pumped through the cryogel at a flow rate of 1.0 mL/min for 30 min. The final HSA concentration in the desorption medium was spectroscopically determined. When desorption was achieved, the cryogel was cleaned with 1 M NaOH and then re-equilibrated with 0.02 M phosphate buffer (pH 8.0). The desorption ratio was calculated from the amount of HSA adsorbed on the cryogel and the final HSA concentration in the desorption medium. To test the repeated use of Cu^{2+}-ASPEC column, HSA adsorption–desorption cycle was repeated for 30 times using the same cryogel column.

2.6.2. HSA adsorption from human plasma

HSA adsorption from human plasma with the Cu^{2+}-ASPEC column was also studied. The blood obtained from a healthy human donor was centrifuged at 500 × *g* for 3 min at room temperature to separate the plasma. Ten milliliters of the freshly separated human plasma was diluted two-fold with phosphate-buffered saline (PBS; pH 7.4, NaCl: 0.9%). Then 20 mL of prepared human plasma was pumped through the column (column volume of 5 mL) under recirculation for 1 h. These experiments were conducted at room temperature. The amount of HSA adsorbed was determined by measuring the initial and final concentration of HSA in plasma. To show specificity of the Cu^{2+}-ASPEC column, adsorptions of other proteins, namely fibrinogen (6.6 mg/mL) and γ-globulin (16.1 mg/mL), were also studied at room temperature for 1 h. Total protein concentration was measured using the total protein reagent (Ciba Corning Diagnostics Ltd., Halstead, Essex, UK; Catalog ref. no. 712076) at 540 nm, which was based on Biuret reaction [23]. Chronometric determination of fibrinogen according to the Clauss method on plasma was performed using Fibrinogene-Kit (ref. nos. 68452 and 68582, bioMerieux Laboratory Reagents and Instruments, Marcy-l'Etoile, France) [24]. HSA concentration was determined using Ciba Corning Albumin Reagent (Ciba Corning Diagnostics Ltd.; Catalog ref. no. 229241), which was based on BCG dye method [23]. γ-Globulin concentration was determined from the difference.

2.7. Electrophoresis analyses

Sodium dodecylsulfate-polyacrylamide gel electrophoresis (SDS-PAGE) analyses of the serum samples were performed on 10% separating mini gels (9 cm × 6.5 cm) and 6% stacking gels for 120 min at 100 V. Gels were stained with 0.25% (w/v) Coomassie Brillant R 250 in acetic acid–methanol–water mixture (1:3:6, v/v/v) and destained in ethanol–acetic acid–water mixture (1:4:6, v/v/v).

3. Results and discussion

3.1. Characterization studies

Aliphatic, aromatic, hydroxyl, carbonyl/carboxyl and ether functional groups are the major binding sites for incorporation of metal ions to the sporopollenin polymeric structure. The amount of chelated Cu^{2+} on SP was measured as 14.1 mg/g SP. Investigation of leakage of Cu^{2+} ions from the SP detected no leakage in any of the adsorption and desorption media, suggesting that the washing procedure was satisfactory for the removal of the nonspecific adsorbed Cu^{2+} ions from the SP. The SEM images of the internal structures of the PHEMA cryogel and Cu^{2+}-attached SP embedded PHEMA cryogel are shown in Fig. 2. Poly(HEMA-SP) cryogel has large continuous interconnected pores (10–50 μm in diameter) with thin polymer walls that provide channels for the mobile phase to flow through. As seen in figure, Cu^{2+}-ASP were uniformly distributed into the PHEMA cryogel network. Pore size of the matrix is much larger than the size of the protein molecules, allowing them to pass easily. HSA has molecular size of 4.0 nm × 4.0 nm × 14.0 nm with an ellipsoidal shape. As a result of the convective flow of the solution/human plasma through the pores, the mass transfer resistance is practically negligible.

The porosity, φ, and the total water content, TWC, of the cryogel column embedded with Cu^{2+}-ASP were measured with deionized water as 67.8% and 90.5% (v/v), respectively. These results indicate that, about 22.7% of the total water was bound by the small pores of polymer matrix where almost no flowing liquid passed through.

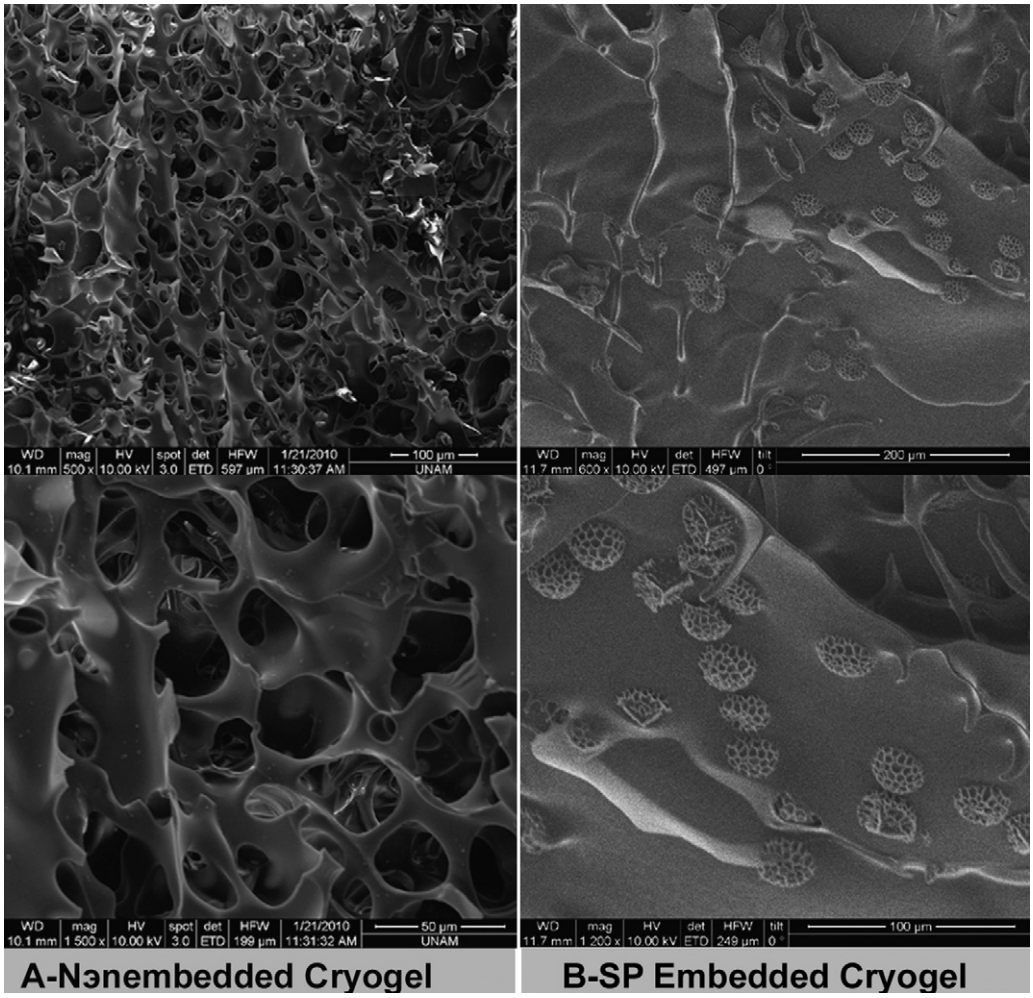

Fig. 2. SEM images of poly(HEMA-SP) cryogel.

However, the large pores constituting 67.8% of the total pores were filled with free water and, most of the fluid flowing channels were taken place within these large pores.

3.2. HSA adsorption from aqueous solutions

3.2.1. Effects of pH

Fig. 3 shows the effect of pH on the adsorption of HSA on Cu^{2+}-ASPEC. The maximum adsorption of HSA was observed at pH 8.0. Above and below pH 8.0, the HSA adsorption capacity decreased.

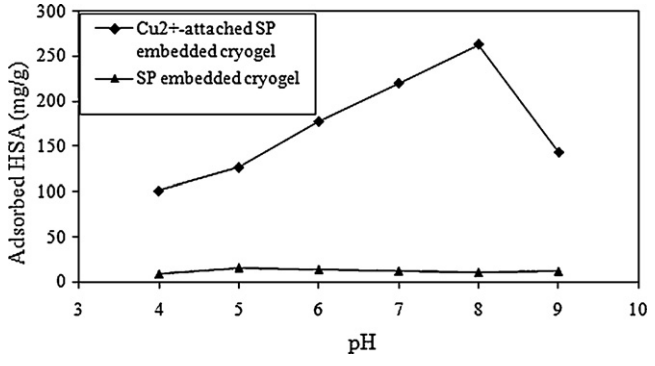

Fig. 3. Effect of pH on HSA adsorption. Embedded SP: 10 mg, HSA concentration: 0.5 mg/mL, flow rate: 1 mL/min, *T*: 25 °C.

The protein adsorption on IMAC is mainly based on chelating bonding between metal ions and amino acid residues. The ionization of amino acid residues at a weakly alkaline pH favors the reaction and therefore induces protein adsorption on the metal-immobilized matrixes [25]. The HSA adsorption in IMAC is mainly through chelation between metal ion and histidine residue of HSA, and the pK_a values of histidine residue in most of proteins are in the range of 6–7 [26–28].

Therefore, the optimal pH for HSA adsorption on Cu^{2+}-ASPEC is around 8.0. It should be also noted that nonspecific adsorption (i.e., adsorption on plain SP embedded cryogel) was independent of pH and it was almost observed the same at all pH values studied.

3.2.2. Effects of HSA concentration

Fig. 4 shows the HSA adsorption isotherm of the plain SP embedded cryogel and Cu^{2+}-ASPEC. HSA adsorption on plain cryogel was low (about 31.5 mg/g SP), although HSA adsorption on Cu^{2+}-ASPEC through Cu^{2+} ions was significant (up to 676.6 mg/g SP). It is noted that, adsorption capacity of this cryogel column is 27.1 mg/g and 4.5 mg/mL, when compared with the mass and bed volume of cryogel column, respectively.

In an adsorption process, the presence of functional groups on polymer and the accessibility of the functional groups without sterical hindrance which is greatly determined by the polymeric matrices are significant parameters. Hydrophilicity and macroporous structures of the polymer are also the best characteristics for

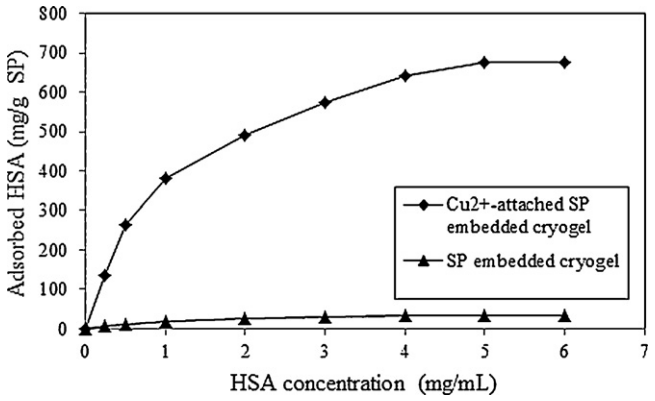

Fig. 4. Effect of HSA concentration on adsorption. pH 8.0, embedded SP: 10 mg, flow rate: 1 mL/min, *T*: 25 °C.

a sorbent [29]. Sporopollenin's porous, hydrophilic structure shows good permeability and functionality depending on stokes' radius of the molecules [12,30].

3.2.3. *Effect of embedded Cu^{2+}-ASP amount*

Effect of HSA adsorption capacities on different Cu^{2+}-ASP amounts embedded to cryogel is shown in Fig. 5. It was found that HSA adsorption capacity of Cu^{2+}-ASPEC was improved significantly due to the embedded Cu^{2+}-ASP amount up to 262.2 mg. As seen in figure that the amount of adsorbed HSA increased with the increasing amount of embedded Cu^{2+}-ASP because of higher surface area [10].

3.2.4. *Adsorption isotherms*

The Langmuir adsorption isotherm was used to characterize the interactions of each protein molecule with the adsorbent. This showed a relationship between the concentration of protein in the solution and the amount of protein adsorbed on the solid phase when the two phases were at equilibrium. The Langmuir adsorption model assumes that molecules are adsorbed at a fixed number of well-defined sites, each of which can hold only one molecule. These sites are also assumed to be energetically equivalent and distant from each other so that there is no interaction between molecules adsorbed on adjacent sites.

Langmuir adsorption isotherm is expressed by Eq. (3). The corresponding transformations of the equilibrium data for HSA gave rise to a linear plot, indicating that the Langmuir model could be applied in these systems and described by the equation:

$$\frac{d_q}{dt} = k_1 C_{eq}(q_m - q_{eq}) - k_2 q_{eq} \tag{3}$$

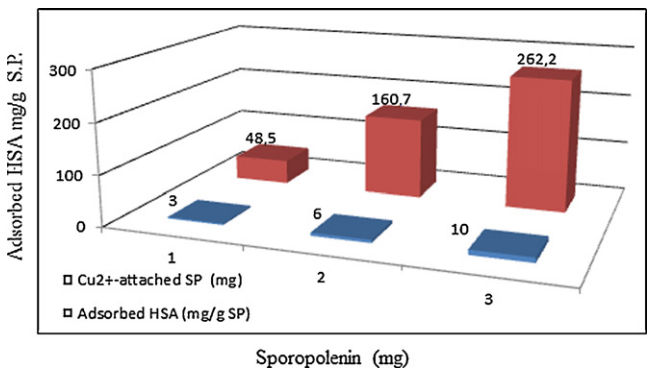

Fig. 5. Effect of embedded Cu^{2+}-ASP amounts on adsorption. HSA concentration: 0.5 mg/mL, pH 8.0, flow rate: 1 mL/min, *T*: 25 °C.

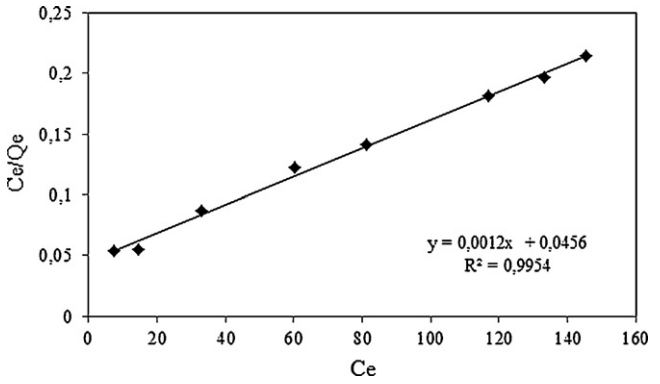

Fig. 6. Linear representation of Langmuir equation of HSA with Cu^{2+}-ASPEC column.

where q_{eq} is the adsorbed amount of HSA (mg/g), C_{eq} is the equilibrium HSA concentration (mg/mL), $K_d = k_2/k_1$ is the dissociation constant of the system, q_m is the maximum adsorption capacity (mg/g). At equilibrium, Eq. (3) can be reduced to the adsorption isotherm:

$$q_{eq} = \frac{q_m C_{eq}}{K_d + C_{eq}} \tag{4}$$

The semireciprocal plot of C_{eq} versus C_{eq}/q_{eq} was employed (Fig. 6). The semireciprocal transformation of the equilibrium data gave rise to a linear plot with a correlation coefficient (R) of 0.9954 for Cu^{2+}-ASPEC, indicating that the Langmuir model could be applied to these affinity adsorbent systems. From the slope and the intercept of the straight line obtained, the values of K_d and q_m are determined. In an ideal adsorbent, the K_d values should be small for the target molecules. The maximum adsorption capacity (q_m), and K_d were found to be 833.3 mg/g SP and 5.67×10^{-4} M for the HSA adsorption on Cu^{2+}-ASPEC, respectively.

3.2.5. *Adsorption kinetics modeling*

In order to examine the controlling mechanism of adsorption process such as mass transfer and chemical reaction, kinetic models were used to test experimental data [31]. The kinetic models (Pseudo-first- and second-order equations) can be used in this case assuming that the measured concentrations are equal to adsorbent surface concentrations. The first-order rate equation of Lagergren is one of the most widely used ones for the adsorption of solute from a liquid solution. It may be represented as follows:

$$\frac{dq_t}{dt} = k_1(q_{eq} - q_t) \tag{5}$$

where k_1 is the rate constant of pseudo-first order adsorption (1/min) and q_{eq} and q_t denote the amounts of adsorbed protein at equilibrium and at time t (mg/g), respectively. After integration by applying boundary conditions, $q_t = 0$ at $t = 0$ and $q_t = q_t$ at $t = t$, gives

$$\log\left[\frac{q_{eq}}{q_{eq} - q_t}\right] = \frac{k_1 t}{2.303} \tag{6}$$

Eq. (6) can be rearranged to obtain a linear form

$$\log(q_{eq} - q_t) = \log(q_{eq}) - \frac{k_1 t}{2.303} \tag{7}$$

a plot of $\log(q_{eq})$ versus t should give a straight line to confirm the applicability of the kinetic model. In a true first-order process $\log q_{eq}$ should be equal to the interception point of a plot of $\log(q_{eq} - q_t)$ via t.

Table 1
The first and second order kinetic constants of HSA adsorption on Cu^{2+}-ASPEC column.

Co (mg/mL)	Exp. q_{eq} (mg/g)	First-order kinetic			Second-order kinetic		
		k_1 (1/min)	q_{eq} (mg/g)	R^2	k_2 (g/mg min)	q_{eq} (mg/g)	R^2
0.25	135.3	0.09972	168.3	0.938	0.000593	163.9	0.996
0.5	262.8	0.11308	385.1	0.911	0.000295	322.6	0.996
1.0	380.6	0.11538	563.5	0.889	0.000223	454.5	0.996
2.0	490.5	0.12644	803.5	0.888	0.00018	588.2	0.995
3.0	575.1	0.13887	1047.1	0.905	0.000145	714.3	0.996
4.0	642.8	0.14440	1148.1	0.915	0.000152	769.2	0.997
5.0	676.6	0.14647	1174.9	0.928	0.000171	769.2	0.996

In addition, a pseudo second order equation based on equilibrium adsorption capacity may be expressed in the form

$$\frac{dq_t}{dt} = k_2(q_{eq} - q_t)^2 \quad (8)$$

where k_2 (g/mg min) is the rate constant of pseudo first order adsorption process. Integrating Eq. (8) and applying the boundary conditions, $q_t = 0$ at $t = 0$ and $q_t = q_t$ at $t = t$, leads to

$$\left[\frac{1}{q_{eq} - q_t}\right] = \left(\frac{1}{q_{eq}}\right) + k_2 t \quad (9)$$

or equivalently for linear form

$$\frac{t}{q_t} = \frac{1}{k_2\, q_{eq}^2} + \left(\frac{1}{q_{eq}}\right) \quad (10)$$

a plot of t/q_t versus t should give a linear relationship for the applicability of the second order kinetics. The rate constant (k_2) and adsorption at equilibrium (q_{eq}) can be obtained from the intercept and slope, respectively.

According to the values in Table 1, the optimum results are for both the second and first order models, with the second order mechanism R^2 values being the highest. These results suggest that the pseudo-second order mechanisms are predominant and that chemisorption might be the rate-limiting step that controls the adsorption process. The rate-controlling mechanism may vary during the course of the adsorption process three possible mechanisms may be occurring [32]. There is an external surface mass transfer or film diffusion process that controls the early stages of the adsorption process. This may be followed by a reaction or constant rate stage and finally by a diffusion stage where the adsorption process slows down considerably [33].

3.2.6. Effect of flow-rate

The adsorption amounts of HSA at different flow-rates are given in Fig. 7. Results show that the HSA adsorption capacity on Cu^{2+}-ASPEC decreases when the flow-rate through the column increases. The adsorption capacity decreased significantly from 355.2 to 169.1 mg/g SP polymer with the increase of the flow-rate from 0.5 to 4.0 mL/min. An increase in the flow rate reduces the solution volume treated efficiently until breakthrough point and therefore decreases the service time of cryogel column. This is due to decrease in contact time between the HSA molecules and Cu^{2+}-ASPEC at higher flow rates. These results are also in agreement with those referred to the literature [34]. When the flow-rate decreases the contact time in the column is longer. Thus, HSA molecules have more time to diffuse to the pore walls of cryogel and to bind to the ligand, hence a better adsorption capacity is obtained. In addition, for column operation the cryogel is continuously in contact with a fresh protein solution. Consequently the concentration in the solution in contact with a given layer of cryogel in a column is relatively constant.

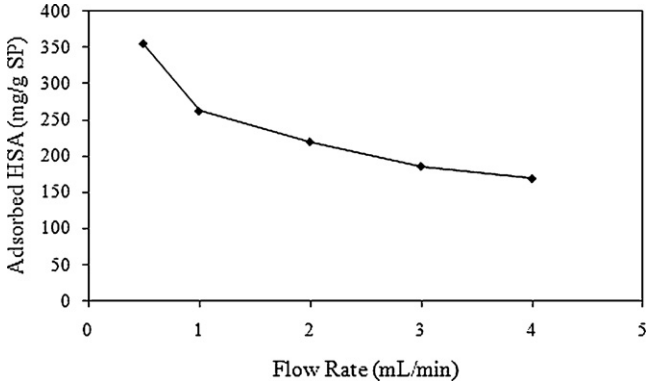

Fig. 7. Effect of flow rate on HSA adsorption. pH 8.0, HSA concentration: 0.5 mg/mL, embedded Cu^{2+}-ASP: 10 mg, T: 25 °C.

3.2.7. Effect of temperature

The effect of temperature on HSA adsorption was studied in the range of 5–35 °C. The equilibrium adsorption of HSA on Cu^{2+}-ASPEC decreased significantly with increasing temperature, and maximum adsorption achieved at 5 °C (Fig. 8). From 5 °C to 35 °C, the adsorption capacity of the cryogel decreased about 26.3% for Cu^{2+}-ASPEC. This behavior can be explained with the exothermic nature of the adsorption process.

3.2.8. Desorption and reusability of adsorbents

Desorption of HSA from Cu^{2+}-ASPEC was also carried out in column system. The desorption of HSA is expressed in percentage of totally adsorbed HSA. Due to economic restraints, there is a growing interest in the preparation and use of effective low-cost and reusable adsorbents [35]. Up to 96.3% of the adsorbed HSA was desorbed using 0.05 M acetate buffer containing 1 M NaCl (pH 5.0) as elution agent. The addition of elution agent reduced electrostatic interactions, resulting in the release of the HSA molecules from the adsorbent. Note that there was no Cu^{2+} release from the cryogel. With the desorption data given earlier, we concluded that 0.05 M acetate buffer containing 1 M NaCl (pH 5.0) is a suitable desorption agent, and allows repeated use of the affinity cryogel used in this study. To show the reusability of Cu^{2+}-ASPEC,

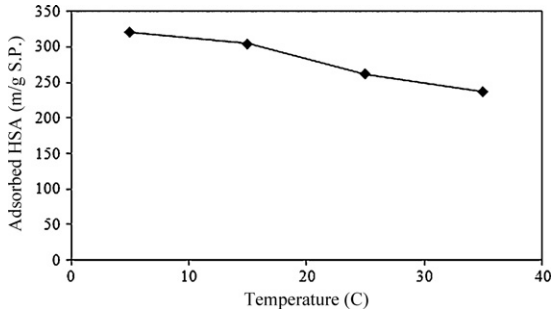

Fig. 8. Effect of temperature on HSA adsorption. pH 8.0, HSA concentration:0.5 mg/mL, embedded Cu^{2+}-ASP: 10 mg, flow rate: 1 mL/min.

Table 2
HSA adsorption from plasma of healthy human donor. Embedded SP: 10 mg, flow rate: 1 mL/min, *T*: 25 °C.

HSA concentration (mg/mL)	HSA adsorbed[a] (mg/g)
5.1	646.50 ± 10.3
10.1	710.31 ± 11.9
20.7	745.93 ± 11.1
27.5	762.65 ± 14.7
41.5	775.42 ± 15.3

[a] Each data is average of five parallel studies.

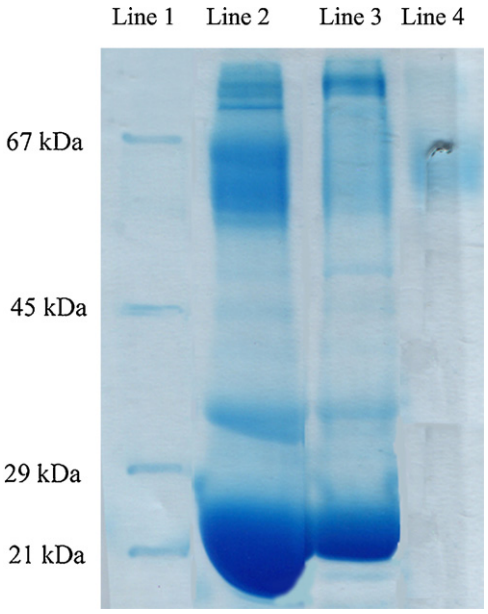

Fig. 9. SDS/PAGE of plasma fractions: Lane 1, biomarker; Lane 2, 1:10 diluted plasma; Lane 3, 1:10 diluted adsorbed plasma. Lane 4, desorbed HSA. Equal amounts of sample were applied to each line.

the adsorption–desorption cycle was repeated 30 times using the same cryogel. There was no remarkable reduction in the adsorption capacity of the cryogel. The HSA adsorption capacity decreased only 6.5% after 30-cycle.

3.3. *HSA adsorption from human plasma*

Table 2 shows the adsorption for human plasma obtained from a healthy donor. There was a low non-specific adsorption of HSA (35.4 mg/g SP) on plain SP embedded cryogel, while much higher adsorption values (775.42 mg/g SP) were obtained when the Cu^{2+}-ASPEC was used. It is worth noting that adsorption of HSA from human plasma on Cu^{2+}-ASPEC was higher than those obtained in studies in which aqueous solutions were used. This may be explained as follows. The high HSA concentration within their native environment (i.e., human plasma) may also contribute to this adsorption capacity due to the high driving force between the aqueous and solid phases. Adsorption of other proteins, namely fibrinogen and γ-globulin, was also obtained as 6.6 and 16.1 mg/g SP, respectively. The total protein adsorption was determined as 813.3 mg/g SP. It is worth noting that the adsorption of both fibrinogen and γ-globulin on Cu^{2+}-ASPEC is negligible. It should also be noted that albumin is the most abundant protein in plasma. It generally makes up more than half of the total plasma proteins. It could be concluded that this low adsorption of fibrinogen and γ-globulin is due to the high concentration of albumin.

In order to confirm that adsorption occurred, before and after albumin adsorbed plasmas were analyzed by SDS PAGE, and the results are shown in Fig. 9. As seen in this figure, protein bands in SDS/PAGE confirm the adsorption of albumin from plasma.

4. Conclusions

Cryogels are one of the novel generations of stationary phases in the separation technology. But, in addition to several advantages such as large pores, short diffusion path, low pressure drop, and very short residence, cryogels have some disadvantages (i.e., low adsorption capacity). Embedding process is one of the methods to improve the cause of low adsorption capacity for cryogels by obtaining large surface area. In this study, a novel continuous supermacroporous monolithic cryogel embedded with Cu^{2+}-ASP was prepared. Due to the large surface area and high protein capacity of these particles, the protein adsorption capacity of the cryogels was significantly improved. As a result, this adsorbent having high adsorption capacity may be a useful tool in the protein separation technology.

References

[1] M.M. Wilkes, R.J. Navickis, Ann. Intern. Med. 135 (2001) 149.
[2] E.J. Cohn, L.E. Strong, W.L. Hughes, D.J. Mulford, J.N. Ashworth, M. Melin, H.L. Taylor, J. Am. Chem. Soc. 68 (1946) 459.
[3] J.F. Stotz, C. Rivat, C. Geschier, P. Colosett, F. Streiff, Swiss Biotechnol. 8 (1990) 7.
[4] V. Karakoc, E. Yılmaz, D. Türkmen, N. Öztürk, S. Akgöl, A. Denizli, Int. J. Biol. Macromol. 45 (2009) 188.
[5] M. Odabaşı, R. Say, A. Denizli, Mater. Sci. Eng. C 27 (2007) 90.
[6] M.B. Ribeiro, M. Vijayalakshmi, D.T. Balvay, S.M.A. Bueno, J. Chromatogr. B 861 (2008) 64.
[7] A. Derazshamshir, B. Ergün, M. Odabaşı Hacettepe, J. Biol. Chem. 35 (2007) 143.
[8] M. Odabaşı, B. Garipcan, A. Denizli, J. Appl. Polym. Sci. 90 (2003) 2840.
[9] M.N. Gupta, S. Jain, I. Roy, Biotechnol. Prog. 18 (2002) 78.
[10] M. Odabaşı, G. Baydemir, M. Karataş, A. Derazshamshir, J. Appl. Polym. Sci. 116 (2010) 1306.
[11] T.T. Yip, T.W. Hutchens, Mol. Biotechnol. 1 (1994) 151.
[12] N. Ünlü, M. Ersoz, J. Hazard. Mater. B 136 (2006) 272.
[13] B.P.H. Binks, J. Clint, G. Mackenzie, C. Simcock, C.P. Whitby, Langmuir 21 (2005) 8161.
[14] S. Wilmesmeier, S. Steuernagel, R. Wiermann, Z. Naturforsch. 48 (1993) 697.
[15] C. Babaç, H. Yavuz, I.Y. Galaev, E. Pişkin, A. Denizli, React. Funct. Polym. 66 (2006) 1263.
[16] A. Hanora, I. Savina, F.M. Plieva, V.A. Izumrudov, B. Mattiasson, I.Y. Galaev, J. Biotechnol. 123 (2006) 209.
[17] A. Derazshamshir, B. Ergün, G. Peşint, M. Odabaşı, J. Appl. Polym. Sci. 109 (2008) 2905.
[18] P. Persson, O. Baybak, F.M. Plieva, I.Y. Galaev, B. Mattiasson, B. Nilsson, A. Axelsson, Biotechnol. Bioeng. 88 (2004) 224.
[19] N. Bereli, G. Şener, E.B. Altıntaş, H. Yavuz, A. Denizli, Mater. Sci. Eng. C 30 (2010) 323.
[20] K. Yao, J. Yun, S. Shen, L. Wang, X. He, X. Yu, J. Chromatogr. A 1109 (2006) 103.
[21] G. Baydemir, N. Bereli, M. Andaç, R. Say, I.Y. Galaev, A. Denizli, React. Funct. Polym. 69 (2009) 36.
[22] N. Ünlü, M. Ersöz, J. Hazard. Mater. B 136 (2006) 272.
[23] N. Tietz, W. Textbook of Clinical Chemistry, W.B. Saunders, Philadelphia, 1986, pp. 589.
[24] A. Clauss, Acta Haematol. 17 (1957) 237.
[25] J.W. Wong, R.L. Albriqht, N.H.L. Wanq, Sep. Purif. Method. 20 (1991) 49.
[26] J. Porath, B. Olin, Biochemistry 22 (1983) 1621.
[27] F.H. Arnold, Bio-Technology 9 (1991) 151.
[28] R. Gutiérrez, E.M. Martín del Valle, M.A. Galán, Sep. Purif. Rev. 36 (2007) 71.
[29] G. Kantipuly, S. Katragadda, A. Chow, H.D. Gesser, Talanta 37 (1990) 491.
[30] N. Unlu, M. Ersoz, Sep. Purif. Technol. 52 (2007) 461.
[31] Y.S. Ho, G. McKay, Process Biochem. 34 (1999) 451.
[32] L. Uzun, H. Yavuz, R. Say, A. Ersöz, A. Denizli, Ind. Eng. Chem. Res. 43 (2004) 6507.
[33] S.J. Allen, B. Koumanova, Z. Kircheva, S. Nenkova, Ind. Eng. Chem. Res. 44 (2005) 2281.
[34] E. Valdman, L. Erijman, F.L.P. Pessoa, S.G.F. Leite, Process Biochem. 36 (2001) 869.
[35] M. Odabaşı, N. Özkayar, S. Özkara, S. Ünal, A. Denizli, J. Chromatogr. B 826 (2005) 50.